Site preference and elastic properties of Fe-, Co-, and Cu-doped Ni_2MnGa shape memory alloys from first principles

Chun-Mei Li,[1,2] Hu-Bin Luo,[2] Qing-Miao Hu,[1,2,*] Rui Yang,[2] Börje Johansson,[1,3,4] and Levente Vitos[1,3,5]

[1]*Applied Materials Physics, Department of Materials Science and Engineering, Royal Institute of Technology, Stockholm SE-100 44, Sweden*

[2]*Shenyang National Laboratory for Materials Science, Institute of Metal Research, Chinese Academy of Sciences, 72 Wenhua Road, Shenyang 110016, China*

[3]*Condensed Matter Theory Group, Physics Department, Uppsala University, P.O. Box 516, SE-75120 Uppsala, Sweden*

[4]*School of Physics and Optoelectronic Technology & College of Advanced Science and Technology, Dalian University of Technology, Dalian 116024, China*

[5]*Research Institute for Solid State Physics and Optics, P.O. Box 49, H-1525 Budapest, Hungary*

(Received 11 February 2011; revised manuscript received 13 May 2011; published 11 July 2011)

The site preference and elastic properties of Fe-, Co-, and Cu-doped Ni_2MnGa alloys are investigated by using the first-principles exact muffin-tin orbital method in combination with coherent-potential approximation. It is shown that Fe atom prefers to occupy the Mn and Ni sublattices even in Ga-deficient alloys; Co has strong tendency to occupy the Ni sublattice in all types of alloys; Cu atoms always occupy the sublattice of the host elements in deficiency. For most of the alloys with stable site occupations, both the electron density n and the shear modulus C' can be considered as predictors of the composition dependence of the martensitic transition temperature T_M of the alloys. The physics underlying the composition-dependent C' are discussed based on the calculated density of states.

DOI: 10.1103/PhysRevB.84.024206 PACS number(s): 62.20.fg, 31.15.A−, 75.50.Cc, 64.70.kd

I. INTRODUCTION

Ni_2MnGa-based alloys have drawn much attention in recent years. These alloys undergo both reversible martensitic and magnetic transitions upon changing temperature, which may result in interesting properties such as magnetic field or thermal change induced shape memory effect (SME). Experiments have demonstrated that the martensitic transformation properties of the Ni_2MnGa alloys may change drastically by doping of a fourth element such as Fe, Co, and Cu.[1–9] For example, the substitution of Mn with Fe ($Ni_2Mn_{1-x}GaFe_x$) up to $x = 0.70$ drops the martensitic transition temperature T_M from 200 K to about 120 K,[1] whereas the replacement of Ga by Fe ($Ni_{52.7}Mn_{22.1}Ga_{25.2-x}Fe_x$, $x = 5.3$) increases T_M from 290 K to 440 K.[2] For the Co- and Cu-doped Mn- or Ga-deficient alloys, T_M increases,[3–6] but it decreases if Co or Cu replaces Ni atoms.[2,7,8]

The high-temperature austenite of Ni_2MnGa is of cubic $L2_1$ structure, consisting of four sublattices: sites $(\frac{1}{4}, \frac{1}{4}, \frac{1}{4})$ and $(\frac{3}{4}, \frac{3}{4}, \frac{3}{4})$ are occupied by Ni, $(\frac{1}{2}, \frac{1}{2}, \frac{1}{2})$ by Mn, and (0, 0, 0) by Ga. The site occupation of the alloying atoms in the lattice is one of the fundamental issues to understand the alloying effect on the properties (e.g., magnetics and modulated structure of the martensite) of Ni_2MnGa-based alloys.[10–12] Generally, the alloying atoms are expected to take directly the sublattice on which the host element is in deficiency. For instance, in the Ni-deficient off-stoichiometric Ni_2MnGa, one would expect that the alloying atoms occupy the Ni sublattice. We call this situation "normal" site occupation. However, the "normal" site occupation may not be always energetically favorable. As demonstrated by our previous investigations, in the Ga-rich Ni_2MnGa alloys, the excess Ga atoms occupy solely the Mn sublattice no matter whether Mn is deficient or not.[13] In the Ni-deficient Ga-rich Ni_2MnGa alloy, some of the Mn atoms move to the Ni sublattice so as to make room for the excess Ga atoms. A very similar situation occurs in the $TiNi_{1-x}Zr_x$ system,[14] where we found that Zr atoms prefer the Ti sublattice and expel some Ti atoms to the Ni one. This kind of site occupancy we will refer to as being "abnormal." Therefore, the site occupancy of the alloying atoms in Ni_2MnGa could be very complicated and needs to be elucidated. However, investigations on the site occupation of the alloying atoms in Ni_2MnGa-based alloys have rarely been found.

The number of valence electrons per atom (e/a) has been identified to be closely related to T_M of the alloys: a larger e/a indicates a higher T_M.[15–17] This correlation provides a predictor for the composition-dependent T_M of Ni_2MnGa-based alloys. However, such a correlation breaks down for the Fe-doped Ni_2MnGa alloys. The experiments of Kikuchi *et al.*,[1] Soto-Parra *et al.*,[2] and Liu *et al.*[18] demonstrated that for $Ni_2Mn_{1-x}GaFe_x$, $Ni_{52.5}Mn_{22.3-x}Ga_{25.2}Fe_x$, and $Ni_{50.5}Mn_{25-x}Ga_{24.5}Fe_x$, larger e/a corresponds to lower T_M. Instead of e/a, Chen *et al.* included the effect of volume by relating the density of valence electrons n, defined as

$$n = (e/a \times N)/V_{\text{cell}}, \tag{1}$$

to T_M.[19] Here, V_{cell} is the volume of the unit cell and N is the number of atoms contained in the unit cell. On the other hand, the shear modulus $C' = \frac{1}{2}(C_{11} - C_{12})$ may also serve as the predictor of the composition-dependent T_M. As we reported previously,[13,20] for the off-stoichiometric Ni_2MnGa alloys, a larger C' indicates a lower T_M. In some cases, C' is even better than e/a as the predictor. For example, our recent calculations demonstrated that C' of $Ni_2Mn(Ga_xAl_{1-x})$ increases with decreasing x, in agreement with the lowering experimental T_M.[21] However, e/a of this alloy remains constant with changing x. Therefore, it is interesting to know whether the T_M-C' correlation works for the Fe-doped Ni_2MnGa alloys or not.

 ©2011 American Physical Society

The purpose of the present paper is to determine first the site occupation of Fe-, Co-, and Cu-doped Ni_2MnGa alloys by the use of a first-principles method. Based on the determined site occupation, the alloying effect on the magnetic moments, equilibrium volume, and elastic properties of these alloys are examined, and the correlations between the composition-dependent T_M and the electron density n as well as the shear elastic modulus C' are discussed.

The rest of the paper is arranged as follows: In Sec. II, we describe the first-principles method we used and the calculation details. In Sec. III, the site preferences of Fe, Co, and Cu in three types of off-stoichiometric Ni_2MnGa alloys are determined. In Sec. IV, the magnetic moments of the studied alloys are presented and the magnetic effect on the site occupations is discussed. In Sec. V, the alloying effect on the equilibrium volume is studied. The connection between the electron density containing the volume effect and the experimental T_M is analyzed. In Sec. VI, we calculate the composition-dependent single-crystal elastic constants, and the correlation between C' and T_M is examined for all the studied Fe-, Co-, and Cu-doped alloys. The physics underlying the alloying effect on C' are explored based on the calculated density of states. Finally, we give our remarks on this work in Sec. VIII.

II. METHODS AND CALCULATION DETAILS

All calculations of the present work are carried out by the use of the first-principles method based on density functional theory,[22,23] formulated with the exact muffin-tin orbitals (EMTO).[24–27] The EMTO method is an improved screened Koringa-Kohn-Rostoker (KKR) method,[25] where the one-electron Kohn-Sham equation is solved by the use of a scalar-relativistic Green's function technique. The one-electron potential is represented by optimized overlapping muffin-tin potential spheres. By using the overlapping spheres, one describes more accurately the exact crystal potential, compared to the conventional muffin-tin or non-overlapping approach.[24,28] In combination with the full charge density (FCD) technique for the total energy calculation,[24] the EMTO method is also suitable to describe accurately the total energy with respect to anisotropic lattice distortions. Another important virtue of the EMTO method is that the coherent-potential approximation (CPA) can be conveniently incorporated.[27,29–31] The CPA is one of the few possible approaches to deal with both the chemical and magnetic disorder at the first-principles level. The EMTO-CPA method has been applied successfully in the theoretical study of the thermophysical properties of metallic alloys[24,27,32–36] and complex oxides.[37–40]

In the present self-consistent calculations, the exchange-correlation term is described within the Perdew-Burke-Ernzerhof (PBE) generalized gradient approximation.[41] The EMTO basis sets include s, p, d, and f components. The Green's function is calculated for 32 complex energy points distributed exponentially on a semicircular contour. After carefully optimizing the overlapping potential spheres (R_{mt}), we set $R_{mt}^{\mathrm{Ni}} = 0.95 R_{ws}$ for the atoms on the Ni sublattice and the usual setup $R_{mt} = R_{ws}$ for the other sublattices, where R_{ws} is the Wigner-Seitz radius. In the one-center expansion of the full charge density, the number of components is truncated at 8. The scalar-relativistic and soft-core approximations are employed. The Ni $3d^8 4s^2$, Mn $3d^5 4s^2$, Ga $3d^{10} 4s^2 4p^1$, Fe $3d^7 4s^1$, Co $3d^7 4s^2$, and Cu $3d^{10} 4s^1$ are treated as valence states. The Brillouin zone was sampled by a $17 \times 17 \times 17$ uniform k-point mesh without any smearing technique. Our test calculations show that the selected parameters can ensure an accuracy of 0.005 mRy/atom of the calculations.

The stable site occupation is determined by comparing the free energies ($F = E - TS$, E being the formation energy per atom, S the mixing entropy per atom, and T the temperature) per atom of the alloy with different site occupation configurations. For an alloy with composition $Ni_{2-x}Mn_{1-y}Ga_{1-z}X_{x+y+z}$,

$$E = \tfrac{1}{4}\{E_{\mathrm{tot}} - [(2-x)E_{\mathrm{Ni}} + (1-y)E_{\mathrm{Mn}} + (1-z)E_{\mathrm{Ga}} + (x+y+z)E_X]\} \tag{2}$$

with E_{tot} being the total energy of the unit cell, and E_{Ni}, E_{Mn}, E_{Ga}, and E_X being the total energies per atom of the pure Ni, Mn, Ga, and X in a hypothetical fcc lattice, respectively. The mixing entropy S is evaluated as

$$S = -\frac{1}{4} k_B \sum_{i=1}^{4} [c_i \ln c_i + (1-c_i)\ln(1-c_i)] \tag{3}$$

with c_i being the atomic fraction on each lattice site i and k_B the Boltzmann constant. The contributions of the lattice vibration and electronic temperature are not included in the free energy. At ambient temperature, the effect of electronic temperature is negligible. The contribution of the lattice vibration to the free-energy difference between different site-occupation configurations (ΔF_{ph}) may be estimated by using the high-temperature expansion of the phonon free energy, according to which $\Delta F_{\mathrm{ph}} \approx 3k_B T(\Delta\Theta/\Theta)$ with Θ being the Debye temperature. With this approximation, ΔF_{ph} is typically two orders of magnitude smaller than that from electronic energy so that it is also negligible.[13]

To calculate the single-crystal elastic constants, we first determine the equilibrium volume and the bulk modulus by fitting the calculated total energies versus volume to a Morse function.[42] Then the elastic moduli C' and C_{44} are calculated by the use of volume-conserving orthorhombic and monoclinic deformations, i.e.,

$$\begin{pmatrix} 1+\delta_o & 0 & 0 \\ 0 & 1-\delta_o & 0 \\ 0 & 0 & \frac{1}{1-{\delta_o}^2} \end{pmatrix} \tag{4}$$

and

$$\begin{pmatrix} 1 & \delta_m & 0 \\ \delta_m & 1 & 0 \\ 0 & 0 & \frac{1}{1-{\delta_m}^2} \end{pmatrix}, \tag{5}$$

respectively. Six strains from $\delta = 0$ to $\delta = 0.05$ with intervals of 0.01 were used to calculate the total energies $E(\delta_o)$ and $E(\delta_m)$. The elastic constants C' and C_{44} were obtained by fitting the total energies with respect to δ_o and δ_m

as $E(\delta_o) = E(0) + 2VC'\delta_o^2$ and $E(\delta_m) = E(0) + 2VC_{44}\delta_m^2$, respectively. C_{11} and C_{12} were evaluated from the bulk modulus $B = \frac{1}{3}(C_{11} + 2C_{12})$ and the tetragonal shear constant $C' = \frac{1}{2}(C_{11} - C_{12})$.

III. SITE PREFERENCE

In the present work, for each alloying element X (X = Fe, Co, and Cu), we consider 3 types of compositions: Ni deficient ($Ni_{2-x}MnGaX_x$) (type 1), Mn deficient ($Ni_2Mn_{1-x}GaX_x$) (type 2), and Ga deficient ($Ni_2MnGa_{1-x}X_x$) (type 3), with $x = 0.05$. For each composition, we consider 5 different site-occupation configurations. Taking the Ni-deficient alloy as example, the 5 site-occupation configurations are (A) the "normal" site occupation with x X atoms occupying the Ni sublattice (denoted as X_{Ni}); (B) x X atoms occupying the Mn sublattice (X_{Mn}) and x Mn atoms moving to the Ni sublattice (Mn_{Ni}); (C) x X occupying the Ga sublattice (X_{Ga}) and x Ga atoms moving to the Ni sublattice (Ga_{Ni}); (D) x X occupying the Mn sublattice (X_{Mn}), x Mn atoms moving to the Ga sublattice (Mn_{Ga}), and x Ga atoms moving to the Ni sublattice; (E) x X occupying the Ga sublattice, x Ga atoms moving to the Mn sublattice (Ga_{Mn}), and x Mn atoms moving to the Ni sublattice. The stable site occupation is determined by comparing the free energies F of the 5 different site-occupation configurations. To observe the effects of temperature and magnetism, we also present the formation energies E and E', calculated respectively with and without spin polarization. The relative energies are presented as ΔF, ΔE, and $\Delta E'$, where the energy of the "normal" site-occupation configuration is taken as reference. ΔF measures the relative stability of various site occupations at temperature $T = 300$ K, which is around the critical temperature of the martensitic transition, whereas ΔE and $\Delta E'$ correspond to the relative stability at 0 K in magnetic and nonmagnetic states, respectively.

Listed in Table I are the relative formation energy (ΔE and $\Delta E'$), relative free energy (ΔF), and the magnetic moment (μ_0) of the three types of Fe-, Co-, and Cu-doped Ni_2MnGa alloys. Note that ΔE and ΔF have similar trends against the site-occupation configurations at the temperature of 300 K. Therefore, in the temperature range of interest, the mixing entropy cannot change the relative stability of the site occupations, so comparing the relative formation energy is actually sufficient to determine the stable site occupancy.

For the Fe-doped Ni- and Mn-deficient alloys, the "normal" site-occupation configuration A with Fe occupying the Ni or Mn sublattice is lower in energy than the "abnormal" site-occupation configurations. However, for the Ga-deficient alloy, the energy difference between the site-occupation configurations A ("normal"), B (with Fe atoms occupying the Ni sublattice while some of the Ni atoms are moving to the Ga sublattice), and C (with Fe atoms occupying the Mn sublattice while some of the Mn atoms are moving to the Ga sublattice) are close to the numerical accuracy of our first-principles calculation. Furthermore, for these systems due to the neglected temperature effects our approach is not sufficient to resolve the site preference. At the same time, the small energy differences suggest that these configurations are almost degenerated in energy and may occur simultaneously in the alloys.

For the Co-doped alloy, regardless of the composition of the alloys, the configuration of Co occupying the Ni sublattice has the lowest energy among all configurations investigated, indicating Co atoms prefer strongly the Ni sublattice. That is, the "normal" site-occupation configuration A is the most stable for the Ni-deficient alloy whereas for both Mn- and Ga-deficient alloys, the "abnormal" site-occupation configuration (B) with Ni antisites on the Mn or Ga sublattice is more stable.

In the Cu-doped alloy, Cu atoms always take the sublattice of the deficient component; i.e., the "normal" site-occupation configuration is the most stable one for all 3 types of Cu-doped alloys.

For all the alloys involved in this study, configurations D and E are not stable. The reason is that two kinds of antisites have to be generated in order to achieve the composition balance for these configurations, which cost a lot of energy.

IV. MAGNETIC MOMENTS

Listed also in Table I are the total magnetic moments (μ_0) of the three types of Fe-, Co-, and Cu-doped Ni_2MnGa alloys with 5 different site-occupation configurations. The total magnetic moments differ significantly for different site-occupation configurations. Observing the local magnetic moments of the six types of atoms (shown in Table II), it is found that Mn, Fe, and Co atoms show different magnetic moments when occupying different sublattices: On the Ni, Mn, and Ga sublattices, the magnetic moments of the Mn atoms are roughly $-2.43\mu_B$, $3.37\mu_B$, and $-3.43\mu_B$, respectively; those of the Fe atoms are roughly $1.39\mu_B$, $2.83\mu_B$, and $2.83\mu_B$, respectively; and those of the Co atoms are roughly $1.03\mu_B$, $1.31\mu_B$, and $1.30\mu_B$. The magnetic moments of Mn atoms on the Ni or Ga sublattice tend to be antiferromagnetically coupled with those of Mn atoms on the Mn sublattice (Mn_{Mn}). Mn, Fe, and Co atoms are almost equally magnetized on the Mn and Ga sublattices with magnetic moments significantly larger than those when they occupy the Ni sublattice. This is because the atoms on the Mn and Ga sublattices have the same Ni surroundings and the magnetic interaction is localized, mainly confined in between Ni_{Ni} and Mn, Fe, and Co on the Mn or Ga sublattice. When occupying the three different sublattices, Ni atoms are also spin polarized with local magnetic moments about $0.32\mu_B$ on the Ni sublattice, in comparison with about $0.15\mu_B$ and $0.12\mu_B$ on Mn and Ga sublattices, respectively. Both Ga and Cu have very small magnetic moments and their magnetic moments remain almost unchanged when occupying different sublattices (shown in Table II).

Since the atoms (mainly Mn, Fe, and Co) exhibit different magnetic moments when occupying different sublattices, the magnetic property of these alloys also changes with different site-occupation configurations. Obviously, the site occupancy is also controlled by the complex magnetic interaction besides the chemical interactions. In Table I, the comparison between ΔE from spin-polarized calculations and $\Delta E'$ from non-spin-polarized calculations may roughly show the (static, i.e., 0 K) magnetic effect on the site occupancy. As seen in Table I, for each site-occupation configuration, ΔE is generally very different from $\Delta E'$. Generally, ΔE is larger than $\Delta E'$, which means that the magnetic effect tends to stabilize the normal site-occupation configuration in all of the studied alloys. This

TABLE I. Relative formation energy ΔE and $\Delta E'$ (in mRy/atom) and relative free energy ΔF (in mRy/atom) of Fe-, Co-, and Cu-doped Ni_2MnGa alloys at a temperature of 300 K, taking the formation and free energy of the "normal" site-occupation configuration as reference. A–E denote different site-occupation configurations (see the text). ΔE and $\Delta E'$ are the relative formation energies from spin-polarized and non-spin-polarized calculations, respectively. Also presented in the table are the total magnetic moments μ_0 (in μ_B). Boldface indicates the most stable configuration.

Type	Composition	Site Occupancy	ΔE	$\Delta E'$	ΔF	μ_0
		Fe doped				
1	$Ni_{1.95}MnGaFe_{0.05}$	**A: $(Ni_{0.975}Fe_{0.025})_2MnGa$**	0	0	0	4.01
		B: $(Ni_{0.975}Mn_{0.025})_2(Mn_{0.95}Fe_{0.05})Ga$	0.41	−0.11	0.31	3.79
		C: $(Ni_{0.975}Ga_{0.025})_2Mn(Ga_{0.95}Fe_{0.05})$	1.48	1.34	1.38	4.15
		D: $(Ni_{0.975}Ga_{0.025})_2(Mn_{0.95}Fe_{0.05})(Ga_{0.95}Mn_{0.05})$	1.57	1.27	1.38	3.72
		E: $(Ni_{0.975}Mn_{0.025})_2(Mn_{0.95}Ga_{0.05})(Ga_{0.95}Fe_{0.05})$	1.11	−0.38	0.92	3.80
2	$Ni_2Mn_{0.95}GaFe_{0.05}$	**A: $Ni_2(Mn_{0.95}Fe_{0.05})Ga$**	0	0	0	3.95
		B: $(Ni_{0.975}Fe_{0.025})_2(Mn_{0.95}Ni_{0.05})Ga$	0.38	−0.77	0.26	3.84
		C: $Ni_2(Mn_{0.95}Ga_{0.05})(Ga_{0.95}Fe_{0.05})$	0.74	−0.26	0.64	3.96
		D: $(Ni_{0.975}Fe_{0.025})_2(Mn_{0.95}Ga_{0.05})(Ga_{0.95}Ni_{0.05})$	0.71	−0.74	0.50	3.83
		E: $(Ni_{0.975}Ga_{0.025})_2(Mn_{0.95}Ni_{0.05})(Ga_{0.95}Fe_{0.05})$	1.81	0.53	1.60	3.97
3	$Ni_2MnGa_{0.95}Fe_{0.05}$	A: $Ni_2Mn(Ga_{0.95}Fe_{0.05})$	0	0	0	4.16
		B: $(Ni_{0.975}Fe_{0.025})_2Mn(Ga_{0.95}Ni_{0.05})$	−0.01	−0.49	−0.13	4.03
		C: $Ni_2(Mn_{0.95}Fe_{0.05})(Ga_{0.95}Mn_{0.05})$	−0.06	−0.07	−0.16	3.73
		D: $(Ni_{0.975}Fe_{0.025})_2(Mn_{0.95}Ni_{0.05})(Ga_{0.95}Mn_{0.05})$	0.31	−0.84	0.1	3.65
		E: $(Ni_{0.975}Mn_{0.025})_2(Mn_{0.95}Fe_{0.05})(Ga_{0.95}Ni_{0.05})$	0.37	−0.59	0.16	3.79
		Co doped				
1	$Ni_{1.95}MnGaCo_{0.05}$	**A: $(Ni_{0.975}Co_{0.025})_2MnGa$**	0	0	0	4.00
		B: $(Ni_{0.975}Mn_{0.025})_2(Mn_{0.95}Co_{0.05})Ga$	1.00	−0.50	0.90	3.70
		C: $(Ni_{0.975}Ga_{0.025})_2Mn(Ga_{0.95}Co_{0.05})$	2.00	0.92	1.90	4.03
		D: $(Ni_{0.975}Ga_{0.025})_2(Mn_{0.95}Co_{0.05})(Ga_{0.95}Mn_{0.05})$	1.98	0.85	1.79	3.64
		E: $(Ni_{0.975}Mn_{0.025})_2(Mn_{0.95}Ga_{0.05})(Ga_{0.95}Co_{0.05})$	1.64	−0.65	1.45	3.69
2	$Ni_2Mn_{0.95}GaCo_{0.05}$	A: $Ni_2(Mn_{0.95}Co_{0.05})Ga$	0	0	0	3.86
		B: $(Ni_{0.975}Co_{0.025})_2(Mn_{0.95}Ni_{0.05})Ga$	−0.21	−0.40	−0.33	3.83
		C: $Ni_2(Mn_{0.95}Ga_{0.05})(Ga_{0.95}Co_{0.05})$	0.71	−0.33	0.61	3.84
		D: $(Ni_{0.975}Co_{0.025})_2(Mn_{0.95}Ga_{0.05})(Ga_{0.95}Ni_{0.05})$	0.12	−0.53	−0.09	3.82
		E: $(Ni_{0.975}Ga_{0.025})_2(Mn_{0.95}Ni_{0.05})(Ga_{0.95}Co_{0.05})$	1.83	0.62	1.62	3.86
3	$Ni_2MnGa_{0.95}Co_{0.05}$	A: $Ni_2Mn(Ga_{0.95}Co_{0.05})$	0	0	0	4.06
		B: $(Ni_{0.975}Co_{0.025})_2Mn(Ga_{0.95}Ni_{0.05})$	−0.53	−0.25	−0.65	4.03
		C: $Ni_2(Mn_{0.95}Co_{0.05})(Ga_{0.95}Mn_{0.05})$	0.01	−0.22	−0.09	3.65
		D: $(Ni_{0.975}Co_{0.025})_2(Mn_{0.95}Ni_{0.05})(Ga_{0.95}Mn_{0.05})$	−0.20	−0.60	−0.41	3.63
		E: $(Ni_{0.975}Mn_{0.025})_2(Mn_{0.95}Co_{0.05})(Ga_{0.95}Ni_{0.05})$	0.43	−0.74	0.22	3.71
		Cu doped				
1	$Ni_{1.95}MnGaCu_{0.05}$	**A: $(Ni_{0.975}Cu_{0.025})_2MnGa$**	0	0	0	3.97
		B: $(Ni_{0.975}Mn_{0.025})_2(Mn_{0.95}Cu_{0.05})Ga$	0.43	−1.28	0.33	3.61
		C: $(Ni_{0.975}Ga_{0.025})_2Mn(Ga_{0.95}Cu_{0.05})$	1.02	0.63	0.92	3.97
		D: $(Ni_{0.975}Ga_{0.025})_2(Mn_{0.95}Cu_{0.05})(Ga_{0.95}Mn_{0.05})$	1.41	0.08	1.22	3.61
		E: $(Ni_{0.975}Mn_{0.025})_2(Mn_{0.95}Ga_{0.05})(Ga_{0.95}Cu_{0.05})$	0.71	−1.05	0.52	3.56
2	$Ni_2Mn_{0.95}GaCu_{0.05}$	**A: $Ni_2(Mn_{0.95}Cu_{0.05})Ga$**	0	0	0	3.77
		B: $(Ni_{0.975}Cu_{0.025})_2(Mn_{0.95}Ni_{0.05})Ga$	0.36	0.39	0.24	3.78
		C: $Ni_2(Mn_{0.95}Ga_{0.05})(Ga_{0.95}Cu_{0.05})$	0.28	0.24	0.18	3.77
		D: $(Ni_{0.975}Cu_{0.025})_2(Mn_{0.95}Ga_{0.05})(Ga_{0.95}Ni_{0.05})$	0.69	0.43	0.48	3.77
		E: $(Ni_{0.975}Ga_{0.025})_2(Mn_{0.95}Ni_{0.05})(Ga_{0.95}Cu_{0.05})$	1.36	1.04	1.15	3.79
3	$Ni_2MnGa_{0.95}Cu_{0.05}$	**A: $Ni_2Mn(Ga_{0.95}Cu_{0.05})$**	0	0	0	3.98
		B: $(Ni_{0.975}Cu_{0.025})_2Mn(Ga_{0.95}Ni_{0.05})$	0.40	0.19	0.28	3.97
		C: $Ni_2(Mn_{0.95}Cu_{0.05})(Ga_{0.95}Mn_{0.05})$	0.38	−0.55	0.28	3.57
		D: $(Ni_{0.975}Cu_{0.025})_2(Mn_{0.95}Ni_{0.05})(Ga_{0.95}Mn_{0.05})$	0.73	−0.18	0.52	3.58
		E: $(Ni_{0.975}Mn_{0.025})_2(Mn_{0.95}Cu_{0.05})(Ga_{0.95}Ni_{0.05})$	0.81	−1.06	0.60	3.64

result is consistent with our finding in off-stoichiometric Ni_2MnGa alloys.[13]

Furthermore, the trends of ΔE and $\Delta E'$ against the site-occupation configurations differ from each other. For example, the site-occupation configuration A of the Fe-doped Mn-deficient alloy is the most stable from spin-polarized calculations whereas configuration B becomes the most stable one from non-spin-polarized calculations. An exception is that

TABLE II. The local magnetic moments (in μ_B) of Ni, Mn, Ga, Fe, Co, and Cu atoms on the three different sublattices Ni, Mn, and Ga. The error is induced by the variation of the compositions and site-occupation configuration.

	Ni	Mn	Ga	Fe	Co	Cu
Ni	0.32 ± 0.02	-2.43 ± 0.06	-0.03	1.39 ± 0.05	1.03 ± 0.02	0.04
Mn	0.15 ± 0.02	3.37 ± 0.02	-0.01	2.83 ± 0.01	1.31 ± 0.03	-0.03
Ga	0.12 ± 0.03	-3.43 ± 0.02	-0.05	2.83 ± 0.02	1.30 ± 0.09	-0.01

ΔE and $\Delta E'$ of the Cu-doped Mn-deficient alloy have similar trends against the site-occupation configurations.

V. EQUILIBRIUM VOLUME

Using the determined stable site-occupation configurations, we investigated the change of equilibrium volume with respect to the composition x ($0 \leqslant x \leqslant 0.2$) for the three types of Fe-, Co-, and Cu-doped Ni_2MnGa alloys, as shown in Fig. 1. With the addition of the Fe, Co, or Cu, the equilibrium volume V_0 (per atom) of the alloy changes linearly with x. For the Fe- and Co-doped alloys, no matter which one of Ni, Mn, or Ga is in deficiency, V_0 decreases with increasing x. Cu doping increases V_0 of the Ni-deficient alloys but decreases V_0 of the Mn- and Ga-deficient alloys. The variation of the equilibrium volume is mainly ascribed to the size difference between the host (1.24 Å, 1.32 Å, and 1.40 Å for the measured atomic radius of Ni, Mn, and Ga, respectively) and alloying elements (1.27 Å, 1.25 Å, and 1.28 Å for Fe, Co, and Cu, respectively). However, there are two exceptions: The atomic radii of Fe and Co atoms are slightly larger than that of Ni, but V_0 of Fe- and Co-doped Ni-deficient alloys decreases with increasing Fe or Co content. This indicates that besides the atomic size, there must be some other factors, such as magnetic effect, affecting the change of volume with respect to the composition.

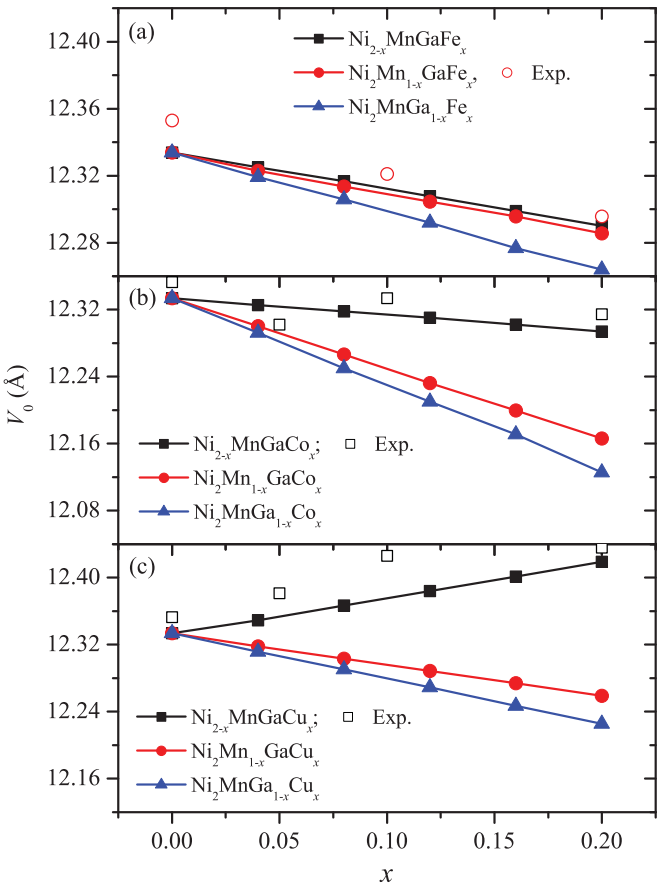

FIG. 1. (Color online) The equilibrium volume V_0 (in Å^3) per atom of Fe- (a), Co- (b), and Cu-doped (c) Ni_2MnGa alloys. The empty squares denote the available experimental data. They are from Refs. 1,7 and 8, respectively, for the three types of alloys: $Ni_2(Mn_{1-x}Fe_x)Ga$, $(Ni_{2-x}Co_x)MnGa$, and $(Ni_{2-x}Cu_x)MnGa$.

In Fig. 1, we also present the available experimental volumes. The trends of the theoretical equilibrium volumes are in general agreement with the experimental findings.[1,7,8] For $Ni_2Mn_{1-x}GaFe_x$, both theoretical and experimental volume decreases linearly with increasing x. However, for $Ni_{2-x}MnGaCo_x$ and $Ni_{2-x}MnGaCu_x$, the linearity of the experimental $V_0 \sim x$ relationship is not as good as the theoretical one, which might be due to the uncertainty in the experimental measurement.

It has been widely recognized that the e/a can be considered a predictor of the composition dependence of martensitic transformation temperature T_M: Larger e/a corresponds to higher T_M.[15–17] However, for some of the alloys, this correlation fails. It has been argued that the volume of the alloys may also be important when tracing T_M. To include the volume effect, Chen *et al.* proposed the electron density n, defined as $n = (e/a \times n_1)/V_{\text{cell}}$ with n_1 being the average number of atoms contained in the unit cell with volume of V_{cell}, to describe the composition dependence of T_M. For the off-stoichiometric Ni_2MnGa alloys, larger n corresponds to higher experimental T_M.[19]

Here, in order to examine the correlation between T_M and n in the Fe-, Co-, and Cu-doped alloys, we collected the experimental T_M[1–9,18,43–45] of some alloys which match roughly the three types of alloys involved in this study. The volume of these alloys are obtained from the linear $V_0 \sim x$ relationship as shown in Fig. 1. In Fig. 2, we plot the T_M as functions of the electron density n. Similar to most of the off-stoichiometric Ni_2MnGa alloys, with increasing n, T_M increases for most of the studied alloys except for the Fe-doped Mn-deficient alloy [shown in Fig. 2(a)]. It is noted that the violation of the $T_M \sim n$ relationship does not occur for all the Fe-doped alloys. The Fe-doped Ga-deficient alloy still follows the larger n-higher T_M rule. The doping effect of Fe on the T_M is generally less significant than that of Co. Especially for the Ni-deficient alloy, Co doping changes T_M drastically: A slight increase in n leads to a very large increase in T_M.

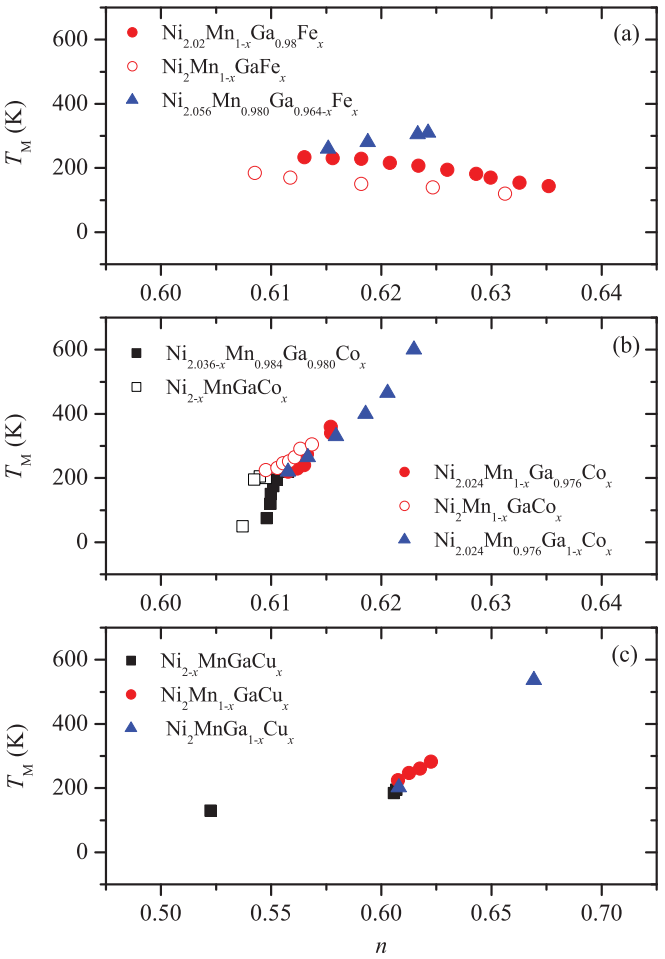

FIG. 2. (Color online) The experimental martensitic transformation temperature T_M with respect to the electron density n $[= (e/a \times n_1)/V_{\text{cell}}$, with n_1 being the average number of atoms contained in the unit cell with volume of $V_{\text{cell}}]$ for the three types of Fe- (a), Co- (b), and Cu-doped (c) Ni_2MnGa alloys. The experimental T_M values are from Refs. 1–9,18,43–45.

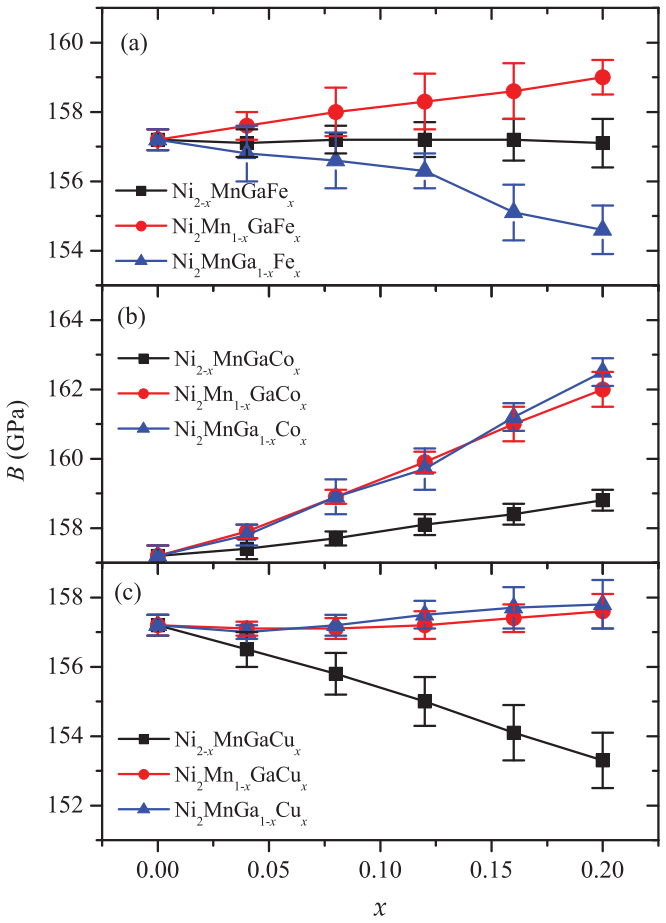

FIG. 3. (Color online) The bulk modulus B (in GPa) of Fe- (a), Co- (b), and Cu-doped (c) Ni_2MnGa alloys.

The failure of the $T_M \sim n$ correlation for some of the Fe-doped Ni_2MnGa alloys might be due to the fact that n is not able to describe the details of the electronic structure of the system. We speculate that the temperature may possibly account for this problem. In the following part of this paper, we discuss this problem in more detail.

VI. ELASTIC PROPERTIES

Based on the stable site-occupation configurations and the equilibrium volume determined in the previous sections, we calculated the single-crystal elastic constants of the three types of Fe-, Co-, and Cu-doped Ni_2MnGa alloys as functions of the composition x. As compared to the equilibrium volume V_0 (Fig. 1), for most of the alloys, the bulk modulus B (Fig. 3) follows the general trend that a larger B corresponds to a smaller V_0. However, both V_0 and B of $Ni_2MnGa_{1-x}Fe_x$ decrease with increasing x, and B of $Ni_{2-x}MnGaFe_{1-x}$ keeps almost constant whereas V_0 decreases. Our previous investigations have shown that C' and C_{44} of the off-stoichiometric Ni_2MnGa alloys change oppositely with the composition.[13,20] Nevertheless, for the Fe-, Co-, and Cu-doped alloys, this is not always true. The trend of C' (Fig. 4) is the same as that of C_{44} (Fig. 5) for $Ni_{2-x}MnGaX_x$ (X = Fe and Co) and $Ni_2Mn_{1-x}GaX_x$ (X = Fe and Cu) alloys.

The martensitic transformation (MT) of Ni_2MnGa-based alloys results from the soft-phonon modes and their accompanying soft tetragonal shear modulus C' of the high-temperature cubic $L2_1$ phase.[46–48] As demonstrated by our previous investigations, for the off-stoichiometric Ni_2MnGa alloys, besides e/a, C' could also be considered as an index of the composition dependence of T_M: A smaller C' indicates a higher T_M.[13,20,21,49–53] Moreover, for $Ni_2Mn(GaAl)$ where the $T_M \sim e/a$ relationship fails, the $T_M \sim C'$ relationship still works.[21] In order to examine the $T_M \sim C'$ of the Fe-, Co-, and Cu-doped alloys, in Fig. 6 we present the experimental T_M as functions of the theoretical C' for some alloys which match roughly the studied three types of alloys. The C' of these alloys are obtained through interpolation of the $C' \sim x$ relationship as shown in Fig. 5. For most of the alloys, T_M decreases with increasing C', following the general trend as for the off-stoichiometric Ni_2MnGa alloys. However, for $Ni_2Mn_{1-x}GaFe_x$, T_M increases with increasing C', against the general trend as happens in the $T_M \sim n$ correlation (see Fig. 2). The sharp change of the T_M of $Ni_{2-x}MnGaCo_x$ with respect to the composition x is also found by observing the $T_M \sim C'$ correlation as in the case of $T_M \sim n$.

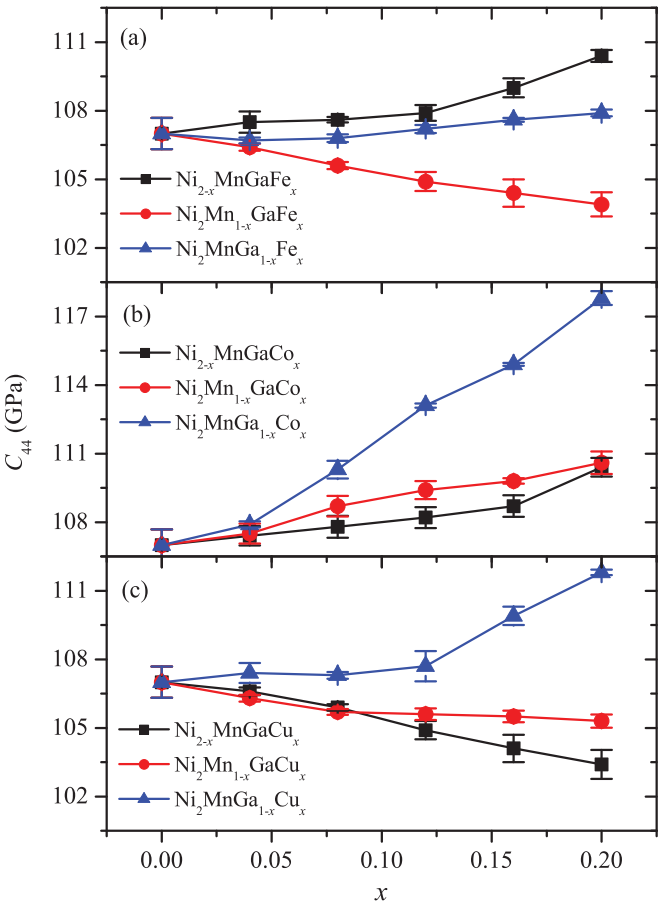

FIG. 4. (Color online) The shear modulus C_{44} (in GPa) of Fe- (a), Co- (b), and Cu-doped (c) Ni_2MnGa alloys.

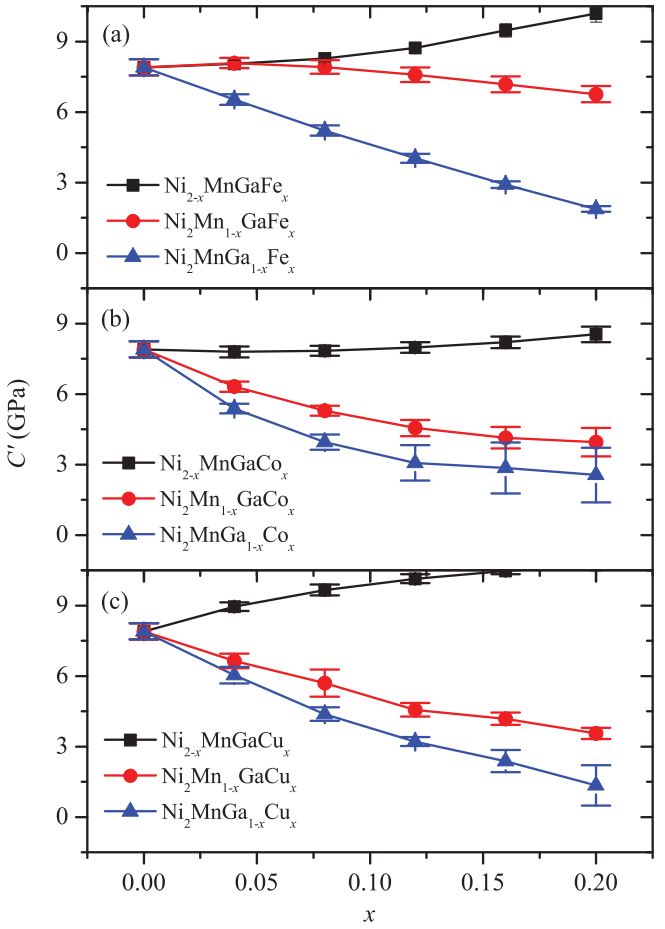

FIG. 5. (Color online) The shear modulus C' (in GPa) of Fe- (a), Co- (b), and Cu-doped (c) Ni_2MnGa alloys.

As shown in Fig. 6, for $Ni_2Mn_{1-x}GaFe_x$ there is an inverse behavior of the $T_M \sim C'$ correlation although C' is expected to be a better predictor of the composition-dependent T_M than n. The reason could be that we are using the 0 K C' to assess the $T_M \sim C'$ correlation. However, in principle, one should use C' around T_M for the $T_M \sim C'$ correlation. The $C' \sim x$ slope for $Ni_2Mn_{1-x}GaFe_x$ at finite temperature might be opposite to that at 0 K which makes this alloy follow the general $T_M \sim C'$ correlation. The strong Co-doping effect for $Ni_{2-x}MnGaCo_x$ might have a similar origin: The $C' \sim x$ slope may increase upon elevating temperature. Our recent investigations on the temperature-dependent C' of $Ni_{2+x}Mn_{1-x}Ga$ show that the density of state smearing induced by temperature changes C' significantly.[54] In the hope of clarifying the violation of the general $T_M \sim C'$ correlation for these alloys, first-principles calculations of the temperature-dependent C' of these alloys are now ongoing.

VII. ELECTRONIC STRUCTURE

Previous investigations have demonstrated that the stability of the $L2_1$ Ni_2MnGa is closely related to the minority (spin-down) density of states (DOS) around Fermi level.[55–57] In order to understand the physics underlying the composition-dependent C', in Fig. 7 we plot the minority DOSs of the Fe-, Co-, and Cu-doped Ni_2MnGa alloys, in comparison with that of the undoped Ni_2MnGa.

For the undoped Ni_2MnGa, there exists a pseudogap at about -0.05 Ry below the Fermi level. This pseudogap forms mainly due to the hybridization between the Ni $3d$ and Ga $4p$ states and represents the covalent bonding between Ni and Ga.[20] On the other hand, a peak occurs at about -0.02 Ry below the Fermi level, resulting in the Jahn-Teller instability of the cubic Ni_2MnGa.[55,57–60] Upon tetragonal distortion, this peak splits, leading to a more stable martensite phase.[55,57–60].

Based on the DOS, the alloying effect on the elastic modulus may be interpreted in terms of the strength of the covalent bonding and the Jahn-Teller effect, noting that the Jahn-Teller effect is directly connected to C' since C' is the elastic modulus of the tetragonal distortion. It is expected that a stronger covalent bond or weaker Jahn-Teller effect should results in harder C'.

As seen from Figs. 7(a), 7(b), and 7(c), for the $Ni_{2-x}MnGaX_x$ (X = Fe, Co, Cu) alloys, the pseudogap at about -0.05 Ry becomes somewhat shallower and narrower as compared to that of the Ni_2MnGa, indicating a weaker covalent bonding between the atoms in the alloys. This may contribute to the softening of the C' of $Ni_{2-x}MnGaX_x$ alloys. However, the peak at about -0.02 Ry is much lower than that of Ni_2MnGa. This means that the Jahn-Teller instability of Ni_2MnGa is significantly relieved by the alloying elements X, which results in the hardening of C'. The calculated weak C' hardening of $Ni_{2-x}MnGaX_x$ with increasing x may be

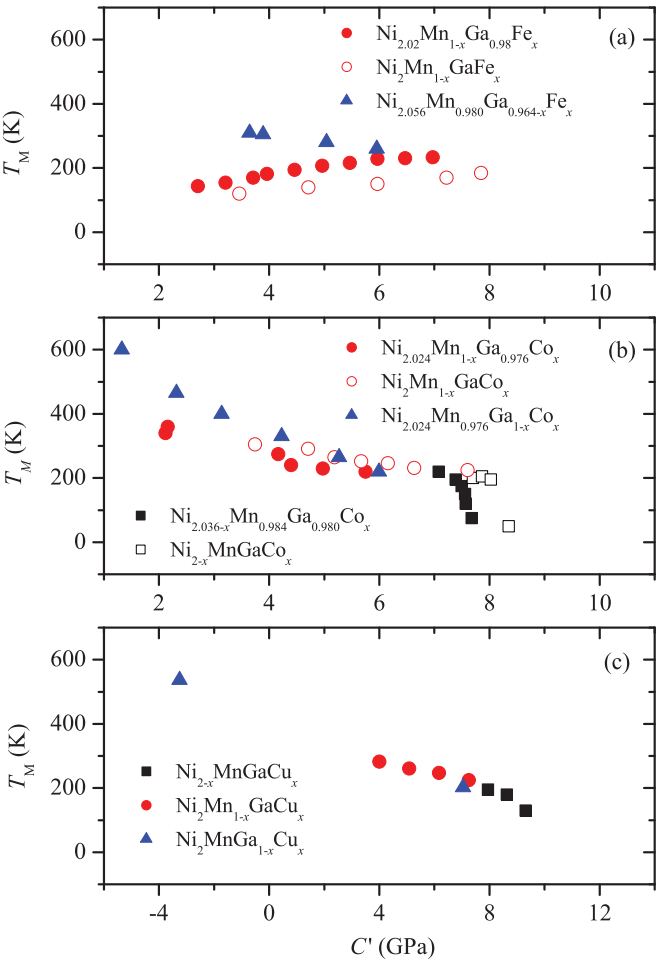

FIG. 6. (Color online) The experimental martensitic transformation temperature T_M with respect to the theoretical shear modulus C' [$= \frac{1}{2}(C_{11} - C_{12})$] for the three types of Fe- (a), Co- (b), and Cu-doped (c) Ni_2MnGa alloys. The experimental T_M values are from Refs. 1–9,18,43–45.

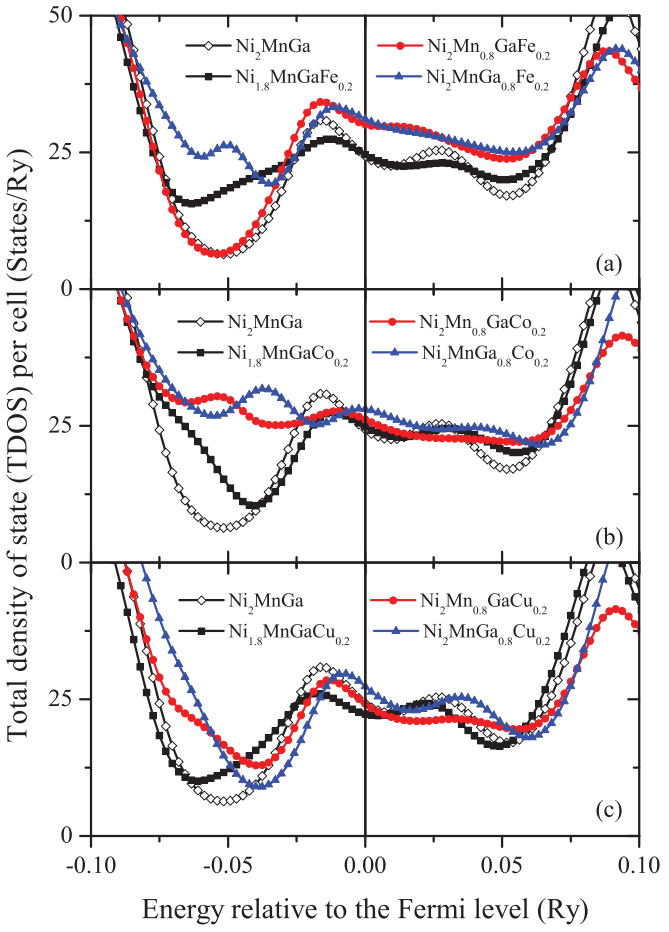

FIG. 7. (Color online) The total density of state (TDOS) per cell of Fe- (a), Co- (b), and Cu-doped (c) Ni_2MnGa alloys, in comparison with that of standard stoichiometric alloy. The vertical lines indicate the Fermi level.

explained as that the C' hardening induced by the Jahn-Teller effect overcomes the softening induced by the covalent bond strength effect.

For the $Ni_2Mn_{1-x}GaFe_x$ alloy, the depth and width of the pseudogap around -0.05 Ry remains almost unchanged whereas the height of the peak at -0.02 Ry increases as compared to that of Ni_2MnGa [see Fig. 7(a)]. Therefore, the contribution of the covalent bond strength effect to the variation of C' is negligible, and the increasing Jahn-Teller instability may account for the softening of C' with increasing x as seen in Fig. 5(a). For the $Ni_2MnGa_{1-x}Fe_x$ alloy, the pseudogap at about -0.05 Ry becomes much shallower and the height of the peak at -0.02 Ry increases, indicating that the covalent bonding becomes weaker and the Jahn-Teller instability increases. Therefore, both the bond strength and Jahn-Teller effects contribute to the softening of C'. This is why the alloying induced C' softening of $Ni_2MnGa_{1-x}Fe_x$ is much more significant than that of $Ni_2Mn_{1-x}GaFe_x$ [see Fig. 5(a)]. For the $Ni_2Mn_{1-x}GaCo_x$ and $Ni_2MnGa_{1-x}Co_x$ alloys, the pseudogap around -0.05 Ry almost disappears [Fig. 7(b)], indicating much weaker covalent bonding in these alloys than that in Ni_2MnGa. The strong weakening of the covalent bonding induced by Co in these alloys results in softening of C' [Fig. 5(b)], although the decrease in the height of the peak at -0.02 Ry (weaker Jahn-Teller effect) may have a positive contribution to the C'. Similar discussion applies to the cases of $Ni_2Mn_{1-x}GaCu_x$ and $Ni_2MnGa_{1-x}Cu_x$ alloys where the covalent bonding becomes weaker and the Jahn-Teller instability is slightly relieved upon Cu doping.

VIII. FINAL REMARKS

Alloying elements affect significantly the martensitic transition and magnetic properties of the Ni_2MnGa-based magnetic shape memory alloys. The site-occupancy of the alloying atoms in the alloy is the basis for the understanding of these effects. Using the first-principles EMTO-CPA method, we determined the site preference of Fe, Co, and Cu in the Ni_2MnGa alloy by comparing the free energies of the alloy with different site-occupation configurations. Our results demonstrated that Fe atoms prefer to occupy the Mn and Ni sublattices even in Ga-deficient alloys; Co has strong tendency to take the Ni sublattice in any type of alloy no matter whether

Ni is deficient or not; Cu always prefers taking the sublattice of the host element in deficiency.

With the determined stable site occupancy, we calculated the electron density n (e/a in unit volume) and elastic modulus of the Fe-, Co-, and Cu-doped Ni_2MnGa. It is found that for most alloys, both n and the shear modulus C' can be considered as predictors of the composition-dependent T_M of the alloys: A larger n or smaller C' corresponds to higher T_M. However, $Ni_2Mn_{1-x}GaFe_x$ is out of the general $T_M \sim n$ and $T_M \sim C'$ correlations. This is not surprising for the $T_M \sim n$ correlation since n contains no electronic structure details of the systems. For the violation of the $T_M \sim C'$ correlation, the reason could be that the temperature effect on C' is not considered in the present work. Based on the calculated density of states, we propose that the composition-dependent C' may be controlled by the interplay between the covalent bond strength and Jahn-Teller effects.

ACKNOWLEDGMENTS

The Swedish Research Council, the Swedish Steel Producers' Association, the Carl Tryggers Foundation, the Göran Gustafsson Foundation, and the Hungarian Scientific Research Fund (research project OTKA 84078) are acknowledged for financial support. The authors also acknowledge the financial support from the MoST of China under Grant No. 2011CB606404 and the NSFC under Grant No. 50871114.

*qmhu@imr.ac.cn

[1] D. Kikuchi, T. Kanomata, Y. Yamaguchi, H. Nishihara, K. Koyama, and K. Watanabe, J. Alloys Compd. **383**, 184 (2004).
[2] D. E. Soto-Parra, X. Moya, L. Mañosa, A. Planes, H. Flores-Zúñiga, F. Alvarado Hernández, R. A. Ochoa-Gamboa, J. A. Matutes-Aquino, and D. Ríos-Jara, Philos. Mag. **90**, 2771 (2010).
[3] M. Khan, I. Dubenko, S. Stadler, and N. Ali, J. Appl. Phys. **97**, 10M304 (2005).
[4] X. Q. Chen, X. Lu, D. Y. Wang, and Z. X. Qin, Smart Mater. Struct. **17**, 065030 (2008).
[5] J. Wang, H. Bai, C. Jiang, Y. Li, and H. Xu, Mater. Sci. Eng. A **527**, 1975 (2010).
[6] J. Wang and C. Jiang, Scr. Mater. **62**, 298 (2010).
[7] T. Kanomata, Y. Kitsunai, K. Sano, Y. Furutani, H. Nishihara, R. Y. Umetsu, R. Kainuma, Y. Miura, and M. Shirai, Phys. Rev. B **80**, 214402 (2009).
[8] T. Kanomata, T. Nozawa, D. Kikuchi, H. Nishihara, K. Koyama, and K. Watanabe, Int. J. Appl. Electro. Mech. **21**, 151 (2005).
[9] D. Soto, F. A. Hernández, H. Flores-Zúñiga, X. Moya, L. Mañosa, A. Planes, S. Aksoy, M. Acet, and T. Krenke, Phys. Rev. B **77**, 184103 (2008).
[10] V. Sánchez-Alarcos, V. Recarte, J. I. Pérez-Landazábal, and G. J. Cuello, Acta Mater. **55**, 3883 (2007).
[11] A. T. Zayak and P. Entel, Mater. Sci. Eng. A **378**, 419 (2004).
[12] M. Gigla, P. Szczeszek, and H. Morawiec, Mater. Sci. Eng. A **438–440**, 1015 (2006).
[13] Q. M. Hu, C. M. Li, R. Yang, S. E. Kulkova, D. I. Bazhanov, B. Johansson, and L. Vitos, Phys. Rev. B **79**, 144112 (2009).
[14] Q. M. Hu, R. Yang, J. M. Lu, L. Wang, B. Johansson, and L. Vitos, Phys. Rev. B **76**, 224201 (2007).
[15] E. C. Do, Y. H. Shi, and B. J. Lee, CALPHAD, Comput. Coupling Phase Diagr. Thermochem. **32**, 82 (2008).
[16] V. Ramamurthy and S. B. Rajendraprasad, J. Phys. Chem. Solids **47**, 1109 (1986).
[17] D. R. Winder and C. S. Smith, J. Phys. Chem. Solids **4**, 128 (1958).
[18] Z. H. Liu, M. Zhang, W. Q. Wang, W. H. Wang, J. L. Chen, and G. H. Wu, J. Appl. Phys. **92**, 5006 (2002).
[19] X. Q. Chen, F. J. Yang, X. Lu, and Z. X. Qin, Phys. Status Solidi B **244**, 1047 (2007).
[20] C. M. Li, H. B. Luo, Q. M. Hu, R. Yang, B. Johansson, and L. Vitos, Phys. Rev. B **82**, 024201 (2010).
[21] Hu-Bin Luo, Chun-Mei Li, Qing-Miao Hu, Rui Yang, Borje Johansson, and Levente Vitos, Acta Mater. **59**, 971 (2011).
[22] P. Hohenberg and W. Kohn, Phys. Rev. **136**, B864 (1964).
[23] W. Kohn and L. J. Sham, Phys. Rev. **140**, A1133 (1965).
[24] L. Vitos, *Computational Quantum Mechanics for Materials Engineers* (Springer-Verlag, London, 2007).
[25] O. K. Andersen, O. Jepsen, and G. Krier, in *Lectures on Methods of Electronic Structure Calculations*, edited by V. Kumar, O. K. Andersen, and A. Mookerjee (World Scientific, Singapore 1994), pp. 63–124.
[26] L. Vitos, H. L. Skriver, B. Johansson, and J. Kollár, Comput. Mater. Sci. **18**, 24 (2000).
[27] L. Vitos, Phys. Rev. B **64**, 014107 (2001).
[28] M. Zwierzycki and O. K. Andersen, Acta Phys. Pol. A **115**, 64 (2009).
[29] P. Soven, Phys. Rev. **156**, 809 (1967).
[30] B. L. Györffy, Phys. Rev. B **5**, 2382 (1972).
[31] L. Vitos, I. A. Abrikosov, and B. Johansson, Phys. Rev. Lett. **87**, 156401 (2001).
[32] L. Vitos, P. A. Korzhavyi, and B. Johansson, Phys. Rev. Lett. **88**, 155501 (2002); Nature Mater. **2**, 25 (2003).
[33] L. Dubrovinsky *et al.*, Nature (London) **422**, 58 (2003).
[34] A. Taga, L. Vitos, B. Johansson, and G. Grimvall, Phys. Rev. B **71**, 014201 (2005).
[35] L. Huang, L. Vitos, S. K. Kwon, B. Johansson, and R. Ahuja, Phys. Rev. B **73**, 104203 (2006).
[36] B. Magyari-Köpe, L. Vitos, and G. Grimvall, Phys. Rev. B **70**, 052102 (2004).
[37] B. Magyari-Köpe, L. Vitos, B. Johansson, and J. Kollár, Acta Crystallogr. Sect. B **57**, 491 (2001).
[38] B. Magyari-Köpe, L. Vitos, B. Johansson, and J. Kollár, J. Geophys. Res. **107**, 2136 (2002).
[39] A. Landa, C.-C. Chang, P. N. Kumta, L. Vitos, and I. A. Abrikosov, Solid State Ionics **149**, 209 (2002).
[40] B. Magyari-Köpe, L. Vitos, G. Grimvall, B. Johansson, and J. Kollár, Phys. Rev. B **65**, 193107 (2002).
[41] J. P. Perdew, K. Burke, and M. Ernzerhof, Phys. Rev. Lett. **77**, 3865 (1996).
[42] V. L. Moruzzi, J. F. Janak, and K. Schwarz, Phys. Rev. B **37**, 790 (1988).

[43]Y. Q. Ma, S. Y. Yang, Y. Liu, and X. J. Liu, Acta Mater. **57**, 3232 (2009).
[44]Y. Q. Ma, S. Y. Yang, W. J. Jin, and X. J. Liu, J. Alloys Compd. **471**, 570 (2009).
[45]P. J. Webster, K. R. A. Ziebeck, S. L. Town, and M. S. Peak, Philos. Mag. B **49**, 295 (1984).
[46]C. Bungaro, K. M. Rabe, and A. Dal Corso, Phys. Rev. B **68**, 134104 (2003).
[47]M. Stipcich, L. Mañosa, A. Planes, M. Morin, J. Zarestky, T. Lograsso, and C. Stassis, Phys. Rev. B **70**, 054115 (2004).
[48]M. Wuttig, L. H. Liu, K. Tsuchiya, and R. D. James, J. Appl. Phys. **87**, 4707 (2000).
[49]F. Falk, Acta Metall. **28**, 1773 (1980); F. Falk and P. Konopka, J. Phys. Condens. Matter **2**, 61 (1990).
[50]O. Nittono and Y. Koyama, Jpn. J. Appl. Phys. **21**, 680 (1982); Y. Koyama and O. Nittono, J. Phys. Colloq. **43**, C4-145 (1982).
[51]J. K. Liakos and G. A. Saunders, Philos. Mag. A **46**, 217 (1982).
[52]G. R. Barsch and J. A. Krumhansl, Phys. Rev. Lett. **53**, 1069 (1984).
[53]X. Ren and K. Otsuka, Mater. Sci. Forum **327-328**, 429 (2000).
[54]C. M. Li, H. B. Luo, Q. M. Hu, R. Yang, B. Johansson, and L. Vitos (unpublished).
[55]C. P. Opeil, B. Mihaila, R. K. Schulze, L. Mañosa, A. Planes, W. L. Hults, R. A. Fisher, P. S. Riseborough, P. B. Littlewood, J. L. Smith, and J. C. Lashley, Phys. Rev. Lett. **100**, 165703 (2008).
[56]A. Ayuela, J. Enkovaara, and R. M. Nieminen, J. Phys. Condens. Matter **14**, 5325 (2002).
[57]P. Entel, V. D. Buchel'nikov, V. V. Khovailo, A. T. Zayak, W. A. Adeagbo, M. E. Gruner, H. C. Herper, and E. Wassermann, J. Phys. D **39**, 865 (2006).
[58]P. J. Brown, A. Y. Bargawi, J. Crangle, K.-U. Neumann, and K. R. A. Ziebeck, J. Phys. Condens. Matter **11**, 4715 (1999).
[59]A. Ayuela, J. Enkovaara, K. Ullakko, and R. M. Nieminen, J. Phys. Condens. Matter **11**, 2017 (1999).
[60]V. V. Godlevsky and K. M. Rabe, Phys. Rev. B **63**, 134407 (2001).